Cyclic response of shallow onshore wind turbine foundations in dense sand

Chisom U Ifeobu, C N Abadie, Stuart Haigh

Geotechnics for Sustainable Infrastructure Development - Geotec Hanoi 2023, Phung (Edt). ISBN

Cyclic response of shallow onshore wind turbine foundations resting on dense sand

Chisom Ifeobu
University of Cambridge, United Kingdom. E-mail: cui20@cam.ac.uk

Christelle Abadie
University of Cambridge, United Kingdom. E-mail: cna24@cam.ac.uk

Stuart Haigh
University of Cambridge, United Kingdom. E-mail: skh20@cam.ac.uk

Keywords: onshore wind, shallow foundation, cyclic loading, centrifuge modelling, lifetime performance

ABSTRACT: Onshore wind plays a central role in the renewable energy mix and will be deployed widely across the globe in the coming years. The foundations typically consist of massive reinforced concrete slabs, designed to resist large moment and lateral loads, but of which the response to repeated cyclic loads of very many cycles is still poorly understood. This paper presents the results of a plane-strain centrifuge model test, aimed at evidencing the behaviour of a typical onshore wind turbine foundation to long-term cyclic loading of increasing magnitude. The results highlight the evolution of the accumulated rotation and settlement of the slab with cycle number and the resulting evolution in deformation mechanism from Particle Image Velocimetry (PIV). The test demonstrates that the slab experiences large rotations, close to the maximum allowable requirements from the current design guidelines. This work provides ground for further investigation towards optimal design to enhance the geotechnical performance while reducing the environmental and financial impact of onshore wind turbine foundations.

1. INTRODUCTION

The world requires about 7 TW of wind energy to achieve net zero emissions by 2050 (IEA, 2022). A significant proportion of this capacity will be provided by onshore wind, with Sub-Saharan Africa playing a major role in the upcoming developments. Shallow raft foundations are the most popular solution to support onshore wind turbines, as they can resist very large overturning moment loads and are relatively straightforward to construct. They typically consist of a 15 – 20 m diameter circular reinforced concrete slab, embedded 2 – 3 m into the ground. These massive structures require colossal quantities of concrete (900 to 1500 m^3) and steel reinforcement (25 tonnes), leading to elevated construction costs and carbon emissions that can be prohibitive for future sustainable development of onshore wind, in particular for developing countries. As a result, cost-effective methods for foundation design that are less material-intensive are needed. This requires rigorous understanding of the lifetime performance of this type of shallow foundation to enable future optimisation.

The design of wind turbine foundations is governed by bearing capacity and tolerance on global rotation. In sand, the constraint on rotation can impose strict restrictions on geometry because of the accumulation of permanent tilt over the lifetime of the turbine. The IEC 61400-6 provides general guidelines for the design of shallow foundations for onshore wind turbines. For ultimate limit state design (ULS), foundation failure is when the maximum load carrying resistance is reached for bearing failure, sliding and overturning as well as considerable settlements or displacements occur under monotonic loading.

Serviceability limit state (SLS) specifies strict allowable settlements and rotations of 25 mm and 0.17 degrees respectively, but little consideration of the response to cyclic wind loading and how to address it is actually provided. It is acknowledged that the accumulation of rotation and settlement

caused by cyclic loading depends on the number of cycles and cyclic load magnitude (Gajan et al.,2005) but this is typically not considered in the current design guidelines.

Current research on the cyclic lateral response of shallow foundations is mostly focused on rocking behaviour under lateral cyclic loading of very few cycle number, relevant to earthquake design. Gajan et al. (2005) performed centrifuge tests involving slow and dynamic cyclic loads on a shallow foundation and demonstrated that permanent settlement of a foundation resting on the soil surface increases with the number of displacement cycles applied, while the rate of settlement accumulation decreases as the footing embeds itself. Gajan and Kutter (2008) found that rotational stiffness depended on the displacement applied with a stiffer response at lower levels of rotation and stiffness degradation at higher rotation levels. However, this work only involves three loading packets with three cycles each and the experiment was displacement controlled. This provides limited data for extension to long-term cyclic loading of very many cycles, typically needed for wind energy applications. In addition, the work does not provide sufficient insight on the failure mechanism.

More recently, Moradi et al. (2023) studied the rocking mechanism of shallow foundations under displacement controlled two-way cyclic loads at 1*g*, and using Particle Image Velocimetry to evidence the failure mechanism. They evidenced the deformation mechanisms in the loading portion of the loading cycle. This consists of soil densification at a depth, involving a wedge mechanism, which causes soil to be pushed away from the slab. This dominates under low rotation conditions and is superseded by a scoop mechanism, which occurs when there are substantial foundation rotations and a considerable gap between the footing and the soil. However, the tests were performed at 1g and do not involve very many cycles (6 cycles).

As a result, there is limited understanding of the foundation response to long-term cyclic moment and lateral loading. To date, this uncertainty in the design has been addressed by using large safety factors, leading to over-engineered foundations. To remedy this problem, an in-depth understanding of the response to long-term wind loading is required.

The present paper investigates the response of a raft foundation in dense sand for a 2 MW onshore wind turbine to cyclic lateral loads at height using centrifuge modelling. The aim is to quantify the accumulation of settlement and rotation of a conventional wind turbine foundation simply resting on dry sand, and subjected to a series of long-term lateral cyclic loads of increasing magnitude. This study provides a worst-case scenario to which current and future optimised designs can be benchmarked against.

2. EXPERIMENTAL METHODOLOGY

2.1 Test set-up

The centrifuge test presented in this paper was performed at an enhanced gravity of 100*g* on the Turner beam centrifuge at the Schofield Centre of

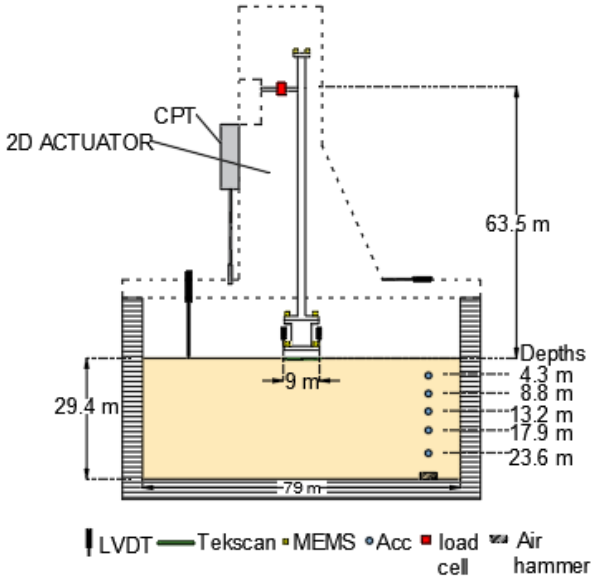

(a)

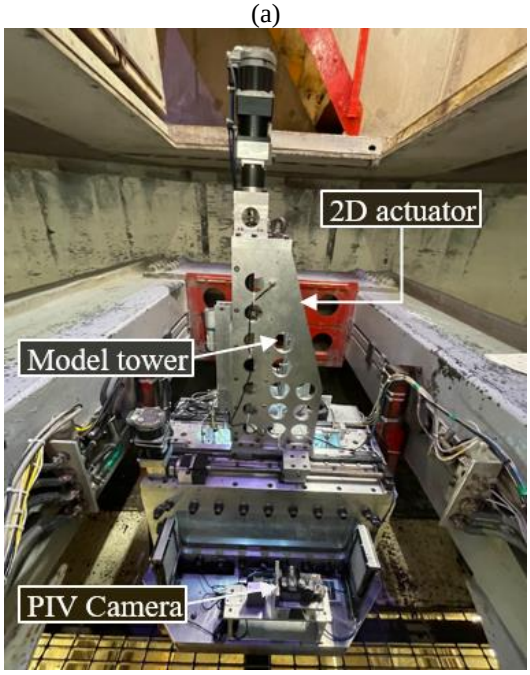

(b)

Figure 1. (a) Cross-section of centrifuge model. Dimensions at prototype scale. MEMS: Microelectro-mechanical systems accelerometer; Acc: Piezoelectric accelerometer, (b) Photo of centrifuge model

the University of Cambridge. The cross-section of the model, with all relevant dimensions, is shown in Figure 1(a), with a photo of the model loaded onto the centrifuge beam in Figure 1(b). Centrifuge modelling enables reduced scale model tests to be performed while preserving stress–strain behaviour of the soil. This is achieved by scaling up the gravity field by a factor of N, with N = 100 in this paper. A set of scaling factors relates the model to the prototype response, according to the framework from Schofield (1980).

2.2 2D model strip footing

The test models a strip foundation resting on dry dense sand, with dimensions representative of a 2 MW turbine foundation, scaled to plane-strain conditions. A 2 MW turbine is typically supported by a reinforced truncated-conical concrete slab of 15.4 m in diameter and 3 m height. The 2D strip footing selected here, and shown in Figure 2, therefore has a width B = 9 m, length L = 17.8 m and a height h = 2 m at prototype scale. Because the length of the footing is fixed by the plane strain container, the width was chosen so that the prototype would have a similar area of contact as a representative foundation. The height was chosen so that the weight of the overall structure was not excessive compared with real turbines.

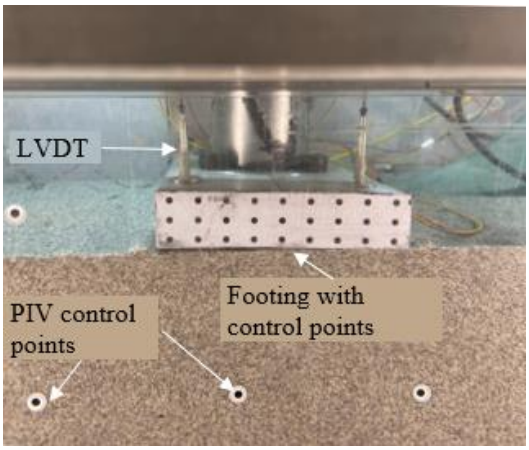

Figure 2. Model strip footing as seen by the camera

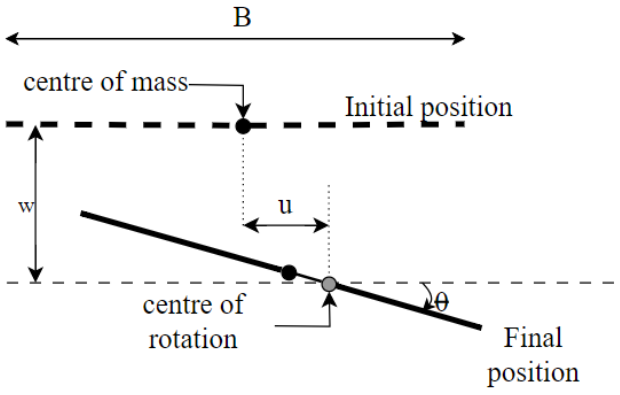

Figure 3: Schematic of key variables used to quantify the foundation movement

Table 1: Hostun sand (HN31) properties (da Silva, 2017).

Property	Symbol	Units	Value
Coefficient of uniformity	C_u	-	1.43
Average particle size	d_{50}	mm	0.356
Minimum void ratio	e_{min}	-	0.555
Maximum void ratio	e_{max}	-	1.010
Specific gravity	G_s	-	2.65
Critical angle of friction	Φ_c	°	35

The movement of the foundation with cycle number was measured in terms of rotation and settlement, as illustrated in Figure 3.

2.3 Sand sample

The model was prepared in a 790 mm x 180 mm x 450 mm container in plane-strain conditions to enable the use of Particle Image Velocimetry (PIV) and further understand the failure mechanism caused by cyclic loads. The sample was prepared using Hostun sand (Table 1), poured at a relative density of D_R=76%. Sand layers were prepared with air pluviation using an automatic sand pourer (Zhao *et al.*, 2006).

2.4 Instrumentation

The soil sample was instrumented using accelerometers to verify the uniformity of the soil stiffness profile, and a cone penetrometer was used to verify the relative density of the sample. A load cell with 250 N capacity (2.5 MN at prototype scale) was used to verify and control the load. Three linear variable displacement transducers (LVDTs) were used to measure the rotation and settlement of the foundation (Figure 1(c). The structure was also instrumented with accelerometers to obtain the rotation. Figure 2 shows a schematic of the key variables used in the following to quantify the foundation movement.

A Canon Powershot G10 Camera with a 14.7 megapixel unit was used to capture soil particles displacements and infer the failure mechanism within the soil through Particle Image Velocimetry (PIV). For this purpose, one third of the sand was died using black ink to increase contrast amongst sand particles. The images were acquired at a frequency of 0.25 Hz. Sand particles displacements were calculated from the recorded images using GeoPIV-RG (Stanier et al., 2015).

2.5 Loading

The footing was subjected to cyclic lateral loads, applied at the top of an aluminum tower at an eccentricity of 63.5 m above the soil surface at

Table 2: Typical design loads for a 2 MW turbine

	H (kN)	M (MNm)	ζ_b	V (MN)
ULS	813	52.9	0.58	11.8
SLS	293	19.0	0.21	11.8

Table 3: Definition of Loading Asymmetry

$\zeta_c = 0$	One-way loading
$\zeta_c = 1$	Two-way loading
$0 < \zeta_c < 1$	Partial one-way loading
$-1 < \zeta_c < 0$	Partial two-way loading

Table 4: Definition of Loading Asymmetry

ID	ζ_b	ζ_c	N
CY1	0.22	0.35	20
CY2	0.30	0.43	20
CY3	0.42	0.36	120
CY4	0.56	0.32	50
CY5	0.45	0.47	10
CY6	0.65	0.25	2
CY7	0.44	0.02	10
CY8	0.57	0.10	10
CY9	0.63	0.02	2
CY10	0.63	-0.03	0.5
Total Number of Cycles for the test:			244.5

prototype scale. The load was applied using a 2D actuator, which enabled to accommodate for vertical settlement during swing-up while applying a cyclic load at the desired eccentricity. A feedback loop, controlled via a load-cell, was implemented to permit repeated cyclic load control of the actuator in the lateral direction. A photo of the model and actuator is provided in Figure 1(b).

The cyclic loading sequence was characterized in terms of load magnitude and amplitude, via the parameters ζ_b and ζ_c, originally defined by Leblanc *et al.* (2010).

$$\zeta_b = \frac{M_{max}}{M_{ult}} \quad (1)$$

$$\zeta_c = \frac{M_{min}}{M_{max}} \quad (2)$$

where M_{max} and M_{min} are the maximum and minimum moment within a load packet respectively, and M_{ult} is the ultimate moment capacity of the footing. The ultimate moment capacity was calculated analytically and represents the limit at which a slab of the same geometry and resting on a hard surface would topple over. This permitted to obtain an immutable value, independent of the soil properties, that could be used to predict the load sequence prior to testing. This simple definition gives the following expression for the ultimate capacity, calculated from a cantilever:

$$M_{ult} = \frac{W_{struc}B}{2} \quad (3)$$

where W_{struc} is the total weight of the model, including the super-structure and the slab. This was calculated to be 66.4 MNm at prototype scale.

Typical design loads for a 2 MW onshore wind turbine foundation is shown in Table 2. The wind loads are based on specifications for the Gamesa G80 2 MW turbine with a hub height of 67 m (The WindPower, 2023). SLS loads were calculated using the rated wind speed of 15 m/s while the ULS loads were calcualted based on the cut out wind speed of 25 m/s. These informed the design of the wind turbine model and the cyclic loading sequence applied.

The wind turbine model weighed 14.7 MN at prototype scale and was similar to the typical vertical design load at full scale. Appropriate values of $\zeta_b$were selected so that the experiment would reflect realistic loading conditions encompassing both the SLS and ULS loading cases.

The loading sequence was selected to apply partial one-way load packets (see definition in Table 2) of increasing load magnitude, representative of severe wind loading on a wind turbine (Table 3, see also later Figure 4(a)). The load magnitude of CY4 is representative of loading at ULS, according to design guidelines. The first and last two cycles of each packet were performed at a much slower rate to permit sufficient sampling for Particle Image Velocimetry. This change in rate is here unlikely to affect the results, as inertial effects are negligible for this type of soil conditions.

3. RESULTS

3.1 General Response

Figure 4 shows the moment-rotation curve for the entire loading sequence. The graph illustrates an

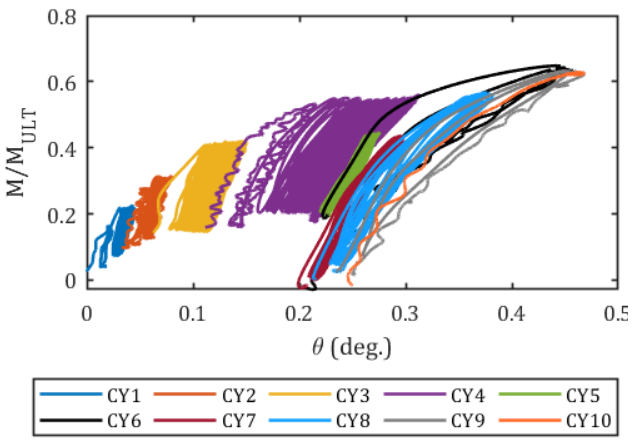

Figure 4. Moment-rotation response of multi-amplitude cyclic test

accumulation of permanent deformation with cycle number, which becomes more prominent as load magnitude increases, due to the increased non-linearity in the soil response. This ratcheting behaviour is commonly observed when studying the cyclic loading response of foundations in dry sand (e.g. Leblanc et al. 2010, Abadie et al. 2019, Richards et al. 2020, Frick & Achmus, 2020).

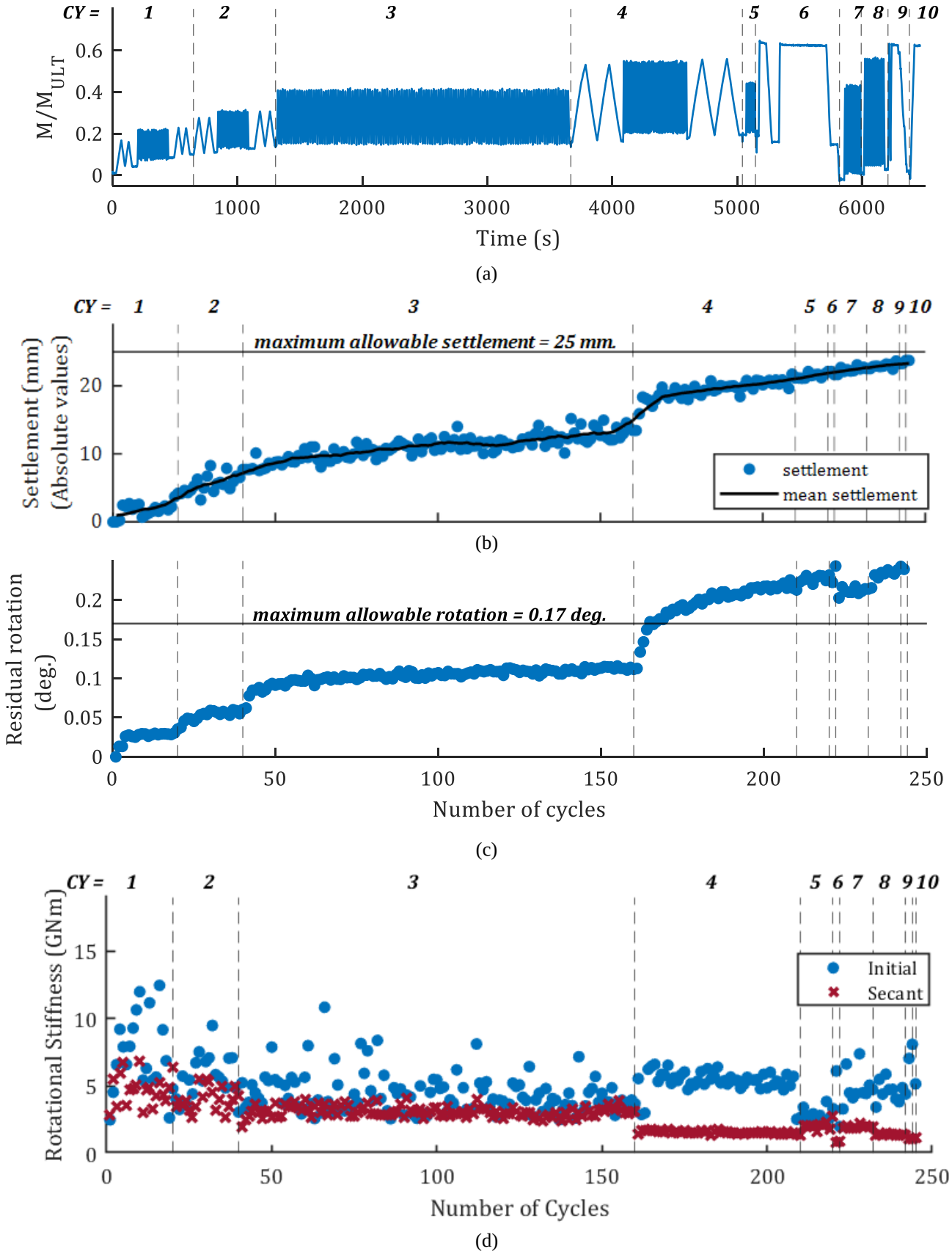

Figure 5. (a) Applied moment history and generated (b) settlement and (c) residual rotation with cycle number (prototype scale). (d) Evolution of the rotational stiffness with cycle number

3.2 *Foundation Displacement*

Figure 5(b) and (c) show the evolution of settlement and residual rotation with cycle number with respect to the cyclic moment sequence applied on top of the foundation (Figure 5(a)). The residual rotation is defined as the rotation at minimum load within a cycle after the foundation has effectively been unloaded. The rate of increase in settlement and rotation with cycle number decreases with the number of cycles within a loading packet and across the entire loading sequence.

The results obtained for this test are compared with the maximum allowable settlement (25 mm) and rotation (0.17 deg.) under Serviceability Limit State (SLS) proposed by the IEC 64100 international standard. The Figures show that these requirements are met at low load levels, close to the elastic regime, but once more severe yielding occurs, the rotation criteria is exceeded and the settlement is close to the tolerated limit. This proves that the design of shallow foundations for onshore wind applications requires careful consideration of the number of cycles and load levels that the slab is likely to experience over its lifetime. Further research is also needed to provide cyclic stability diagrams (Poulos, 1989; Jardine and Standing, 2012), adapted for shallow foundation design.

Figure 6 shows the average footing settlement against its rotation in which positive vertical axis denotes uplift. The results highlight that settlement and rotation are accumulated concurrently, with large settlement and limited rotation accumulated during the cycles of low magnitude, but much larger rotations and more limited settlement generated by the much larger cycles (CY4 onwards). The rate of deformation accumulation is similar from CY1 to CY3, where the cycles are close to the elastic regime

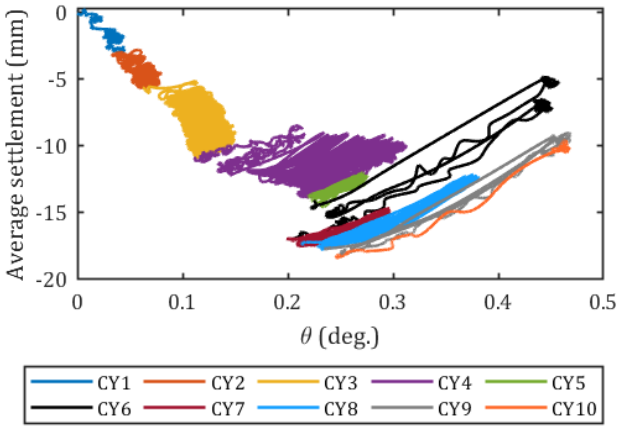

Figure 6. Moment-rotation response of multi-amplitude cyclic test

(see next section and Figure 5(d)). However, further yielding generated by CY4, generates more severe rotation, accumulated at a faster rate than in the previous load packets.

3.3 *Stiffness*

Figure 5(d) compares the initial (tangential) stiffness to the secant rotational stiffness, obtained by measuring the slope from minimum to maximum points within each moment-rotation loading cycle. When both stiffness are super-imposed, this shows that the response is quasi-elastic, which is the case for CY1 to CY3. Beyond this, the soil exhibits a much more pronounced non-linear response, with much greater unrecoverable deformation (Figure 5(b, c), Figure 6). Performing cyclic loads at much smaller amplitudes following a load packet of large amplitude (e.g. CY4 to CY5) typically brings the response back within the yield surface, towards a quasi-elastic response.

Comparing Figure 5(b) and 5(d), there is a marked difference between the rate of increase in settlement for the near-elastic regime (CY1 to CY3, CY5, CY7) and the yielding regime (CY4 and beyond). The rate of settlement and rotation accumulation is unsurprisingly higher after large nonlinear behaviour has been observed.

3.4 *Deformation Mechanisms*

Particle Image Velocimetry was finally used to evidence the deformation mechanism of the soil under the slab during each loading packet. Figure 7 shows the soil displacement vectors and maximum shear strain at the end of the most critical loading packet, CY4.

Large shear strains were observed around the loaded edge. Both a scoop and wedge mechanisms were observed, which concurs with the observations from Moradi et al. 2023, obtained at 1*g*. The soil particles are pushed away from the loaded edge forming the wedge mechanism. Additionally, substantial foundation rotation and gapping beneath the footing produces a scoop mechanism as soil flows to fill the gap formed. Figure 7 also identifies the location of the rotation point, situated at the intersection of the two mechanisms.

4. CONCLUSIONS

This paper describes the long-term lateral cyclic behaviour of a shallow foundation resting on a dense sandy soil. The results show that large settlement and rotations can be accumulated during the lifetime of a foundation, which could potentially reach SLS

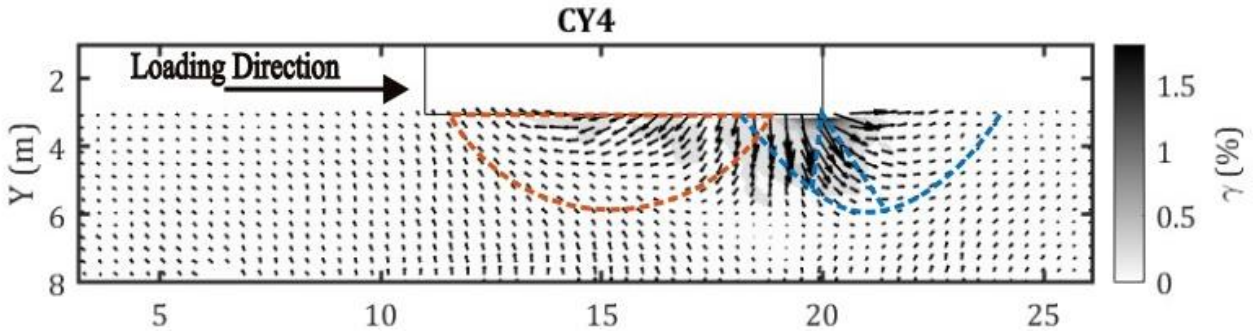

Figure 7. Soil deformation mechanisms at the end of load packet CY4. Displacement field overlain on maximum shear strain contours. Note that shear strains are calculated relative to the beginning of each loading packet, dimensions are in prototype scale and displacement vectors are not to scale

design limits. Low amplitude cycles produce an increase in settlement caused by the quasi-elastic response of the slab to the moment loads, while larger magnitude cycle produce more significant rotation of the foundation, combined with moderate settlement accumulation.

Cyclic lateral and moment loading of the shallow foundation generate the formation of a wedge mechanism on the passive side of the foundation, while a scoop mechanism forms on the active side, where the slab is most likely to lose contact with the soil. Tracking the evolution of this mechanism can provide the impetus for further understanding of the transition in behaviour of the slab between low-amplitude and large-amplitude loads. This would provide grounds for the development of safety guidelines to ensure that shallow foundations do not exhibit excessive settlement nor rotation during the lifetime of onshore wind turbine, potentially also providing information for lifetime extension of existing structures.

5. ACKNOWLEDGEMENTS

The author is grateful for the generous support of the Cambridge-Africa Scholarship. We are also thankful for the help of the technicians of the Schofield Centre at the University of Cambridge (John Chandler, Kristian Pether, Mark Smith and Chris McGinnie) and the valuable guidance from Prof. Gopal Madabhushi, Dr Chuhan Deng and Douglas Morley.

6. REFERENCES

Abadie, C.N., Byrne, B.W. & Houlsby, G.T. (2019). Rigid pile response to cyclic lateral loading: laboratory tests. *Géotechnique* 69:10, 863-876 https://doi.org/10.1680/jgeot.16.P.325

Anastasopoulos, I., Gelagoti, F., Kourkoulis, R., & Gazetas, G. (2011). Simplified constitutive model for simulation of cyclic response of shallow foundations: validation against laboratory tests. Journal of Geotechnical and Geoenvironmental Engineering, 137(12), 1154-1168. https://doi.org/10.1061/(ASCE)GT.1943-5606.0000534

Frick, D., & Achmus, M. (2020). An experimental study on the parameters affecting the cyclic lateral response of monopiles for offshore wind turbines in sand. *Soils and Foundations*, *60*(6), 1570–1587. https://doi.org/10.1016/j.sandf.2020.10.004

Gajan, S., Kutter, B. L., Phalen, J. D., Hutchinson, T. C., & Martin, G. R. (2005). Centrifuge modeling of load-deformation behavior of rocking shallow foundations. *Soil Dynamics and Earthquake Engineering*, *25*(7–10), 773–783. https://doi.org/10.1016/J.SOILDYN.2004.11.019

Gajan, S., & Kutter, B. L. (2008). Capacity, settlement, and energy dissipation of shallow footings subjected to rocking. Journal of Geotechnical and Geoenvironmental Engineering, 134(8), 1129–1141.https://doi.org/10.1061/(ASCE)1090-0241(2008)134:8(1129)

Gajan, S., & Kutter, B. L. (2009). Contact Interface Model for Shallow Foundations Subjected to Combined Cyclic Loading. Journal of Geotechnical and Geoenvironmental Engineering, 135(3), 407–

419.https://doi.org/10.1061/(ASCE)1090-0241(2009)135:3(407)
IEA (2022), Wind Electricity, IEA, Paris https://www.iea.org/reports/wind-electricity, License: CC BY 4.0
IEC. (2019). IEC 61400-1:2019 (4.0) [International Standard].
Jardine, R. J., & Standing, R. J. (2012). Field axial cyclic loading experiments on piles driven in sand. *Soils and Foundations*, 52(4), 723-736. https://doi.org/10.1016/j.sandf.2012.07.012
Leblanc, C., Byrne, B. W., & Houlsby, G. T. (2010). Response of stiff piles to random two-way lateral loading. Géotechnique, 60(9), 715–721. https://doi.org/10.1680/geot.09.T.011
Moradi, M., Hosseini, S. M. M. M., & Khezri, A. (2023). Investigation of rocking mechanism of shallow foundations on sand via PIV technique. *Earthquake Engineering & Structural Dynamics*, *52*(6), 1762–1784. https://doi.org/10.1002/eqe.3842
Poulos, H. G. (1989). Pile behaviour—theory and application. *Géotechnique*, 365-415 https://doi.org/10.1680/geot.1989.39.3.365
Richards, I. A., Byrne, B. W., & Houlsby, G. T. (2020). Monopile rotation under complex cyclic lateral loading in sand. *Géotechnique*, *70*(10), 916–930. https://doi.org/10.1680/jgeot.18.P.302
Schofield, A.N. 1980. Cambridge Geotechnical Centrifuge Operations. Géotechnique, 30(3), pp. 227–268.
da Silva TS (2017) Centrifuge modelling of the behaviour of geosynthetic-reinforced soils above voids. PhD thesis, University of Cambridge, Cambridge, UK.
Stanier, S. A., Blaber, J., Take, W. A., & White, D. J. (2016). Improved image-based deformation measurement for geotechnical applications. Canadian Geotechnical Journal, 53(5), 727–739. https://doi.org/10.1139/cgj-2015-0253
The WindPower. (2023). Gamesa G80/2000. https://www.thewindpower.net/turbine_en_44_gamesa_g80-2000.php
Zhao, Y. et al. (2006) 'Calibration and use of a new automatic sand pourer', in Physical Modelling in Geotechnics, 6th ICPMG'06 - Proceedings of the 6th International Conference on Physical Modelling in Geotechnics, pp. 265–270.